

# Electrochemical Determination of Rutin on ZIF-8-derived Porous Carbon and Aminated Graphene Nanocomposite Modified Electrode

Meng Jiang<sup>1§</sup>, Lin Zhu<sup>1§</sup>, Zejun Zhang<sup>1</sup>, Yijing Ai<sup>1</sup>, Lina Zeng<sup>2,\*</sup>, Shuhai He<sup>3</sup>, Lin Li<sup>2</sup>, Wei Sun<sup>1,\*</sup>

<sup>1</sup> Key Laboratory of Laser Technology and Optoelectronic Functional Materials of Hainan Province, Key Laboratory of Functional Materials and Photoelectrochemistry of Haikou, College of Chemistry and Chemical Engineering, Hainan Normal University, Haikou 571158, P. R. China

<sup>2</sup> College of Physics and Electronic Engineering, Hainan Normal University, Haikou 571158, P. R. China

<sup>3</sup> Hainan Ecological Environmental Monitoring Center, 98 Baiju Avenue, Haikou 571126, P. R. China

<sup>§</sup>These authors contributed equally to this work.

\*E-mail: [zenglinahainan@126.com](mailto:zenglinahainan@126.com) and [sunwei@hainnu.edu.cn](mailto:sunwei@hainnu.edu.cn)

Received: 13 July 2022 / Accepted: 15 August 2022 / Published: 10 September 2022

---

In this article the ZIF-8 based metal-organic frameworks-derived porous carbon was mixed with aminated graphene to obtain the nanocomposite, which was used to modify the surface of glassy carbon electrode (GCE). SEM, XRD and FT-IR were used to characterize the nanocomposite, which exhibited the unique morphology with functional groups. The modified electrode was applied to the electrochemical detection of rutin. Compared with that of GCE, the current response of rutin increased obviously on the modified electrode. Square wave voltammetry was further applied to quantitative analysis of rutin with a linear relationship between the concentration and peak current in two sections from 0.25 to 0.7  $\mu\text{mol}\cdot\text{L}^{-1}$  and 0.7 to 1.5  $\mu\text{mol}\cdot\text{L}^{-1}$  with detection limit of 15  $\text{nmol}\cdot\text{L}^{-1}$ . Consequently, the detection of real samples was realized by this method.

---

**Keywords:** ZIF-8-derived porous carbon; Aminated graphene; Modified electrode; Rutin

## 1. INTRODUCTION

Nanostructured carbon materials have been received much attentions with wide applications in electrochemical fields to improve the performance [1], such as graphene (GR) [2], carbon fiber [3], diamond [4] and carbon nanotube [5]. Most of the carbon materials have special nanostructures, which can improve the electrochemical property, enhance the conductivity, and provide unique dimensional

effect. More recently, researchers are also interest in investigating on the functional materials including N-doped [5], in-situ growth [6] and nanocomposite [7].

Metal-organic frameworks (MOFs)-derived porous carbon (DPC) is a novel carbon material with the “morphologies in control” conception. Along with the advantages of controllable porosity, good thermal/chemical stability, high electrical conductivity, electrocatalytic activity, easy modification with other elements and materials [8,9], MOF-derived carbon materials can provide efficient catalytic activity [10], intensify gas adsorption/separation process and improve electromagnetic wave absorption properties [11,12]. Due to the wide usage of GR with two-dimensional structure, DPC can be combined with GR to get the nanocomposite with many novel functions. For example, Liu et al. reported MOF-derived N-doped porous carbon coated GR as high-performance anodes for lithium-ion batteries [13]. Zhang et al. used the MOF-derived porous Ni<sub>2</sub>P/GR composite for sensitive nonenzymatic glucose sensing [14]. Xu et al. prepared nitrogen-doped GR quantum dot from MOF-derived porous carbon for selective fluorescence detection of Fe<sup>3+</sup> [15]. The unique structure of the DPC and GR can provide superior electrical conductivity owing to a close contact between porous carbon structure and GR nanosheet to obtain a consecutive conductive network [16], which provides the potential advantages in the field of electrochemistry [17].

As a flavonoid compound with many medical functions such as anti-inflammatory, anti-bacteria, anti-tumor and anti-oxidant, rutin (3',4',5,7-tetrahydroxyflavone 3 $\beta$ -D-rutinoside) have been studied by many researchers. Electrochemical quantitative analysis of rutin has been developed, which utilizes various nanomaterials to modify electrodes with the improved effective surface area and the increase of the current response [18-21]. In this study the excellent electrochemical properties of DPC and aminated GR composite was checked for the quantitative detection of rutin, which showed excellent electrochemical performance with highly selective and sensitive response for the rutin analysis.

## 2. EXPERIMENTAL

### 2.1 Instruments and reagents

Electrochemical measurements were performed on CHI 660D electrochemical workstation (Shanghai Chenhua Instrument, China) and a typical three electrode system. Scanning electron microscopy (SEM) was recorded on a JSM-7100F instrument at 5 kV (JEOL, Japan). X-ray diffraction (XRD) results were carried out on D8 Advance with a Cu K $\alpha$  ( $\lambda=1.5406$  Å) radiation source (Bruker, USA) to reveal the crystal structure. Nicolet 6700 FT-IR spectrometer was used to detect FT-IR data in the wavelength range of 500-4000 cm<sup>-1</sup> (Thermo Fisher Scientific, America).

Aminated graphene (GR-NH<sub>2</sub>) was obtained from Jiangsu XFNANO Materials Tech. Co., Ltd. (China). 2-methylimidazole (2-MIM), Zn(NO<sub>3</sub>)<sub>2</sub>·6H<sub>2</sub>O and N,N-dimethylformamide (DMF) are analytically pure grade and purchased from Shanghai Aladdin Bio-Chem. Tech. Co., Ltd. (China). Phosphate buffer solutions (PBS, 0.1 mol·L<sup>-1</sup>) were used as electrolytes and all solutions were prepared by Ultra-pure water (Milli-Q IQ 7000, Merck Millipore, Germany).

## 2.2 Preparation of MOFs-derived porous carbon (DPC)

ZIF-8 was synthesized by conventional solvothermal method [22]. 50 mL solution containing  $\text{Zn}(\text{NO}_3)_2 \cdot 6\text{H}_2\text{O}$  ( $4.0 \text{ mmol} \cdot \text{L}^{-1}$ ) and 2-MIM ( $16.0 \text{ mmol} \cdot \text{L}^{-1}$ ) was stirred at room temperature for 3 h. Then, the mixture was transferred into a 100 mL Teflon-lined stainless-steel reactor for 4 h at  $120^\circ\text{C}$ . The turbid solution was separated by centrifugation, washed with methanol and DMF, and dried under vacuum at  $80^\circ\text{C}$  for 12 h to obtain ZIF-8. DPC was prepared by annealing of ZIF-8 under a stream of He at  $900^\circ\text{C}$  for 3 h in a tube furnace.

## 2.3 Preparation of GR-NH<sub>2</sub> and DPC composite

Ultrafine suspension of  $1.0 \text{ mg} \cdot \text{mL}^{-1}$  DPC solution was prepared by ultrasonic treatment of DPC in ethanol for 3 h. Then 5 mg GR-NH<sub>2</sub> was added in the DPC suspension and ultrasonic dispersion for another 3 h to obtain GR-NH<sub>2</sub> and DPC suspension solution.

## 2.4 Electrode fabrication

The glassy carbon electrode (GCE,  $\phi = 3.0 \text{ mm}$ ) was polished sequentially with sandpaper and  $0.05 \mu\text{m}$  alumina slurry on polishing cloth to produce a mirror-like surface, and then sonicated for 1 min in distilled water and ethanol, respectively. After that,  $5.0 \mu\text{L}$  GR-NH<sub>2</sub>/DPC suspension was dropped onto the surface of GCE and dried at  $30^\circ\text{C}$  to obtain GR-NH<sub>2</sub>/DPC/GCE, which was used as the working electrode for electrochemical detection of rutin. Other modified electrodes were prepared by the similar procedure for comparison.

# 3. RESULTS AND DISCUSSION

## 3.1 Morphological and structural characterization

The morphologies of DPC and GR-NH<sub>2</sub>/DPC are characterized by SEM. As shown in the Fig. 1, the DPC has a typical hexagonal crystal morphology and exhibits a three-dimensional structure (Fig. 1A). GR-NH<sub>2</sub> has a 3D flexible and conductive interconnected network, which can cover or support the inflexible DPC particles. As shown in the Fig. 1B, SEM images proved that GR-NH<sub>2</sub> presents the stacked folded lamellar structure and DPC was dispersed within the layer structure of GR-NH<sub>2</sub>.

Fig. 1C displays the XRD patterns of ZIF-8, DPC and GR-NH<sub>2</sub>/DPC. ZIF-8 showed the characteristic peaks for planes (001), (002), (112) and (222) that matched the literature results [23], suggesting the successful formation of ZIF-8. The XRD patterns of DPC have peaks at  $22^\circ$  and  $45^\circ$ , owing to the (002) and (101) lattices of the hexagonal graphite carbon after carbonization [24,25]. The peak intensity in the XRD spectrum of GR-NH<sub>2</sub>/DPC is obviously higher than that of DPC, which was due to the abundance of carbon provided by GR and DPC simultaneously.

The surface chemical functional groups of materials can be determined by FT-IR. As for the precursor ZIF-8 (Fig. 1D), the absorption bands at  $3439\text{ cm}^{-1}$  and  $419\text{ cm}^{-1}$  were assigned to the C-H, O-H and Zn-N stretch modes, respectively. The sharp peak at  $2937\text{ cm}^{-1}$  can be attributed to the C-H stretching of imidazole [26]. Peaks at  $1593\text{ cm}^{-1}$  and  $1140\text{ cm}^{-1}$  were C=N and C-N stretching vibrations, respectively [27]. After calcination and transformation into DPC (Fig. 1E), the Zn-N stretch mode disappeared, proved that the Zn ions were reduced to Zn metal and then vaporized in the process of carbonization. Furthermore, the characteristic stretching vibration peak for C=N and C-N at  $1593\text{ cm}^{-1}$  and  $1140\text{ cm}^{-1}$  were still retained, means that N-doped carbon materials had been successfully prepared. As for GR-NH<sub>2</sub>/DPC (Fig. 1F), the observation of the spectrum revealed that the complexation with GR-NH<sub>2</sub> resulted in a slightly blue-shift of the GR-NH<sub>2</sub>/DPC stretching vibration peak due to the interaction with N atom [28].

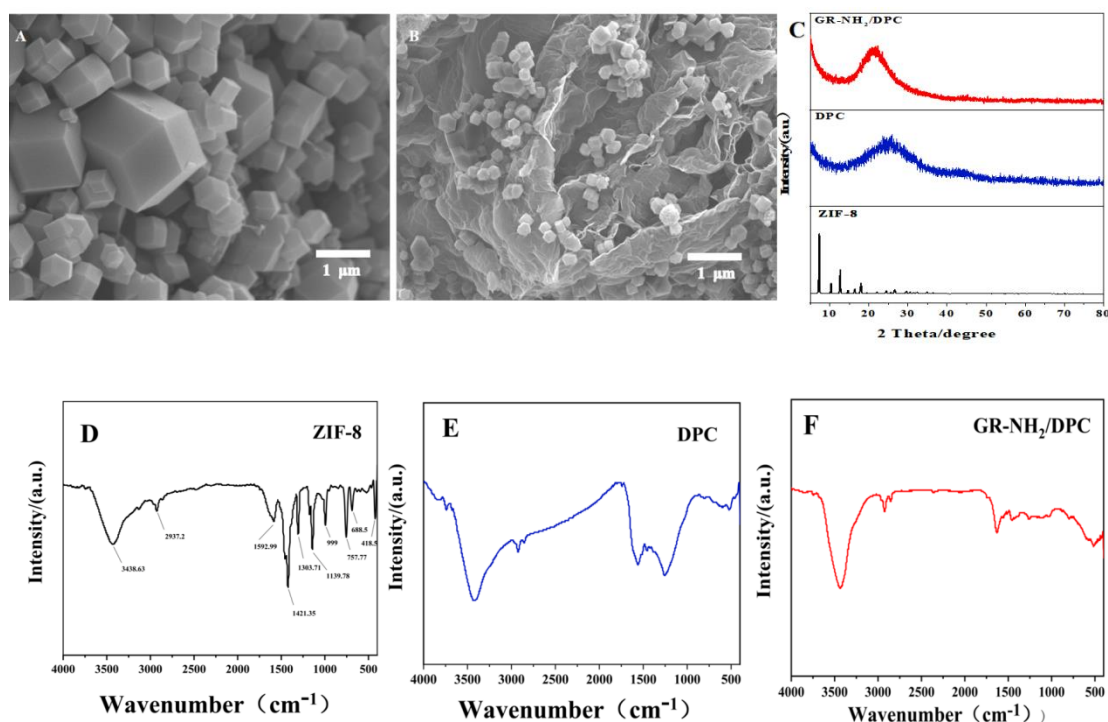


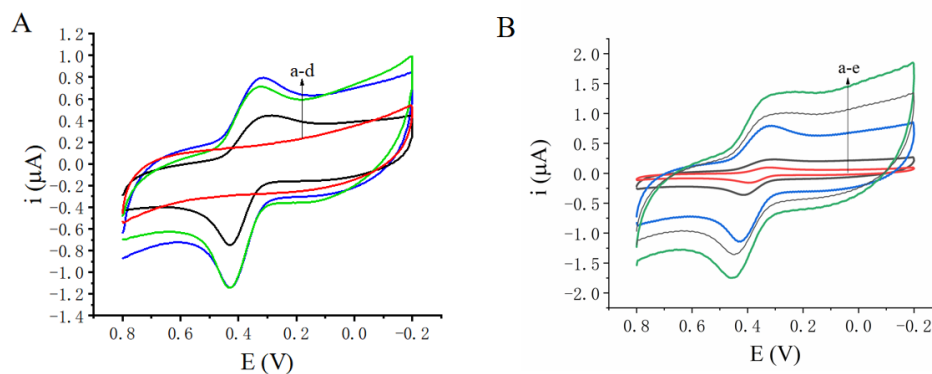
**Figure 1.** SEM images of DPC (A), GR-NH<sub>2</sub>/DPC (B) and XRD patterns of ZIF-8, DPC and GR-NH<sub>2</sub>/DPC(C); FT-IR spectra of ZIF-8 (D), DPC (E) and GR-NH<sub>2</sub>/DPC (F).

### 3.2 Electrochemical behaviors of rutin

The electrochemical responses of  $1.0 \times 10^{-4}\text{ mol}\cdot\text{L}^{-1}$  rutin on different electrodes in  $0.1\text{ mol}\cdot\text{L}^{-1}$  PBS (pH=5) are researched by cyclic voltammetry (CV) and the results are shown in Fig. 2A. It can be seen that a pair of well-defined redox peaks appeared, which was the typical redox reaction of rutin on the electrode due to its electroactive molecular structure [29]. The catechol structure in rutin structure can be oxidized to 3', 4'-diquinone and undergo a reduction reaction on the modified electrode, therefore rutin exhibits good electrochemical activity [30]. In Fig.2A, the redox peak currents on GR-

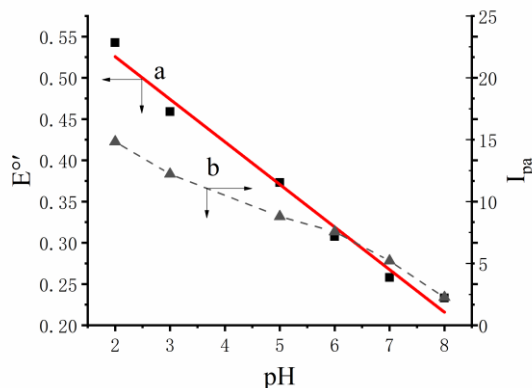
NH<sub>2</sub>/DPC/GCE are more obvious than those on bare GCE, DPC/GCE, GR-NH<sub>2</sub>/GCE. The increased redox peak currents may be attributed to the higher conductivity of DPC and GR-NH<sub>2</sub>, and the synergetic effects of DPC and GR-NH<sub>2</sub> to improve the electron transfer rate and electrochemical responses.

Fig. 2B shows the effect of scan rates (20-1500 mV·s<sup>-1</sup>) on the electrochemical behavior of GR-NH<sub>2</sub>/DPC/GCE in 1.0×10<sup>-4</sup> mol·L<sup>-1</sup> rutin solution. The redox peak currents gradually increased with the increase of scan rate, and the equations were expressed as  $I_{pa}(\mu A) = -8.607v^{1/2}(V \cdot s^{-1}) + 0.058$  ( $r=0.998$ ) and  $I_{pc}(\mu A) = 7.031v^{1/2}(V \cdot s^{-1}) - 0.305$  ( $r=0.992$ ). Thus, the electrochemical reaction of rutin on the modified electrode is a typical diffusion-controlled process, which may be attributed to the high conductive interface of GR-NH<sub>2</sub> and DPC on the electrode. Furthermore,  $E_{pa}$  and  $E_{pc}$  values showed linear correlations with the logarithm of scan rate at higher scan rates. The regression equations were got as  $E_{pa}(V) = 0.032\ln v(V \cdot s^{-1}) + 0.516$  and  $E_{pc}(V) = -0.023\ln v(V \cdot s^{-1}) + 0.382$ . From Laviron's equation, the slopes of  $E_{pa}-\ln v$  and  $E_{pc}-\ln v$  lines are equal to  $RT/(1-\alpha)nF$  and  $-RT/\alpha nF$ , respectively [31]. Therefore, the electron transfer coefficient ( $\alpha$ ) and the electron transfer number ( $n$ ) can be obtained as 0.58 and 1.89 ( $n$  is close to theoretical value of 2). Furthermore, the electron transfer rate constant ( $k_s$ ) could be calculated as 1.50 s<sup>-1</sup>, which is larger than the reported values of 0.33 s<sup>-1</sup> [32], 1.02 s<sup>-1</sup> [33] and 1.24 s<sup>-1</sup> [34]. Therefore, the GR-NH<sub>2</sub> and DPC composite on the GCE surface exhibited high electron transfer rate.



**Figure 2.** (A) Cyclic voltammograms of 1.0×10<sup>-4</sup> mol·L<sup>-1</sup> rutin on (a) GCE, (b) DPC/GCE, (c) GR-NH<sub>2</sub>/GCE, (d) GR-NH<sub>2</sub>/DPC/GCE; (B) cyclic voltammograms of GR-NH<sub>2</sub>/DPC/GCE with different scan rate in pH 5.0 PBS (from a to e are 0.02, 0.1, 0.5, 1.0, 1.5 V·s<sup>-1</sup>) (insert: linear relationship of cathodic and anodic peak current ( $I_p$ ) versus square of sweep rate ( $v^{1/2}$ )).

The influence of pH on electrochemical behaviors of rutin is investigated from 2.0 to 8.0 by CV (Fig. 3). Then, a linear regression equation between  $E^{0'}$  and pH was obtained as  $E^{0'}(mV) = -51.62 \text{ pH} + 65.89$  ( $r=0.992$ ). The slope value of  $-51.62 \text{ mV} \cdot \text{pH}^{-1}$  was close to the theoretical value of  $-59 \text{ mV} \cdot \text{pH}^{-1}$ , implying an equal number of electrons and protons during the rutin redox reaction. Therefore, two electrons are confirmed to be involved in the electrochemical reaction of rutin on GR-NH<sub>2</sub>/DPC/GCE and the electrochemical mechanism can be deduced according to the reference [35] (Fig. 4).



**Figure 3.** The relationship between  $E_0'$  and pH (curve a) and the plot of anodic peak current ( $I_{pa}$ ) versus pH (curve b) in  $1.0 \times 10^{-4} \text{ mol} \cdot \text{L}^{-1}$  rutin.

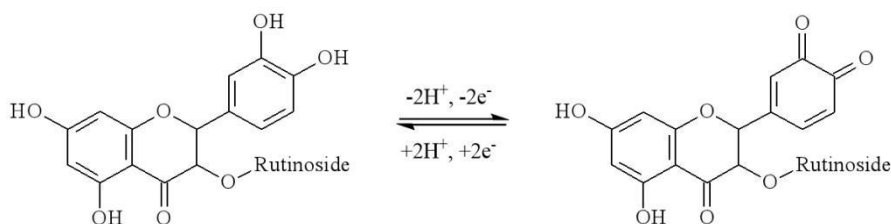


**Figure 4.** The electrochemical mechanism for rutin

### 3.3 Electrochemical detection of rutin on GR-NH<sub>2</sub>/DPC/GCE

Electrochemical detection of rutin was studied by SWV with the instrumental parameters as  $\Delta E_s = 4 \text{ mV}$ ,  $\Delta E_p = 25 \text{ mV}$ ,  $f = 100 \text{ Hz}$ , and the overlapped curves are shown in Fig. 5A. Under the optimized conditions, the anodic current curve of rutin displayed a well-defined symmetrical peak with the  $E_{pa}$  as  $0.406 \text{ V}$  (Fig. 5A). Also the anodic peak currents increased linearly with rutin concentrations in two sections from  $0.25$  to  $0.7 \text{ } \mu\text{mol} \cdot \text{L}^{-1}$  and  $0.7$  to  $1.5 \text{ } \mu\text{mol} \cdot \text{L}^{-1}$  (Fig. 5B) with the linear regression equations as  $I_{pa}(\mu\text{A}) = 4.14 + 5.01C \text{ (mol} \cdot \text{L}^{-1})$  ( $r = 0.99$ ) and  $I_{pa}(\mu\text{A}) = 7.02 + 1.27C \text{ (}\mu\text{mol} \cdot \text{L}^{-1})$  ( $r = 0.99$ ), respectively. The limit of detection (LOD) is got as  $15 \text{ nmol} \cdot \text{L}^{-1}$ . Compared with other modified electrodes for the analysis of rutin (Table 1), the analytical performance of GR-NH<sub>2</sub>/DPC/GCE for rutin is relatively good.

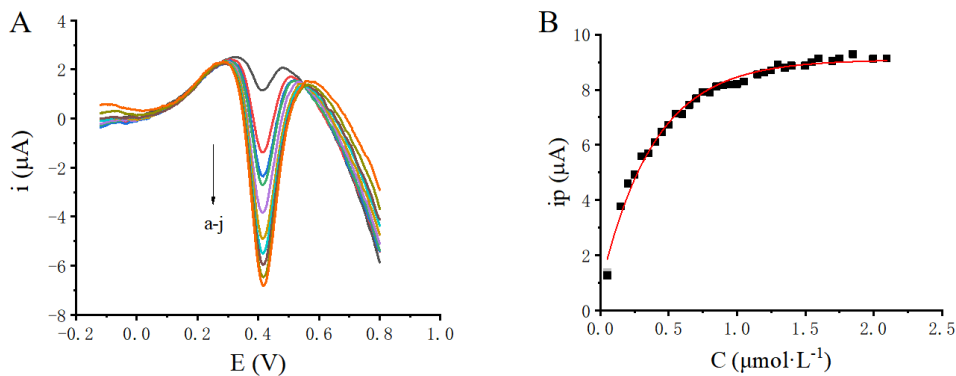


**Figure 5.** SWV curves of different concentration rutin (a to j) 0.05, 0.15, 0.2, 0.25, 0.35, 0.5, 0.65, 0.8, 1.1, 1.5  $\mu\text{mol}\cdot\text{L}^{-1}$  (PBS pH=5.0) on GR-NH<sub>2</sub>/DPC/GCE; (b) linear relationship of rutin concentration and peak current.

**Table 1.** Comparison of analytical parameters of rutin determination with different modified electrodes

Modified electrodes	Methods	Linear range ( $\mu\text{mol}\cdot\text{L}^{-1}$ )	LOD ( $\text{nmol}\cdot\text{L}^{-1}$ )	References
ZnO-AuNPs/rGO/GCE	DPV	0.06-6.0	1.0	[36]
ZIF-67@3D rGA/GCE	DPV	0.05-200.0	1.6	[37]
AuNCs/CILE	DPV	0.004-700.0	1.33	[38]
MnO <sub>2</sub> @FBPC/GCE	DPV	0.008-700.0	2.67	[39]
GDY-IL/GCE	DPV	2.0-150.0	2.7	[40]
ICBG/GCE	DPV	0.08-52.0	11.0	[41]
Ti <sub>3</sub> Al <sub>0.5</sub> Cu <sub>0.5</sub> C <sub>2</sub> /GCE	DPV	0.02-50.0	15.0	[42]
Mg <sub>2</sub> Al-LDH/CILE	DPV	0.08-800.0	25.5	[43]
IL-GR/GCE	DPV	0.03-1.0	10.0	[44]
MWNTs-IL-Gel/GCE	DPV	0.072-6.0	20.0	[45]
GR-NH <sub>2</sub> /DPC/GCE	SWV	0.25-1.5	15.0	This work

### 3.4. Stability and reproducibility

The stability of GR-NH<sub>2</sub>/DPC/GCE were explored with electrochemical response studied over 7 days storage periods, and the peak current only decreased 1.35%, indicating good stability. The relative standard deviations (RSD) for rutin detection were 1.40% (n=5) with five individual electrodes, showing excellent reproducibility.

### 3.4 Interference study

The influences of common co-existing substances on the determination of rutin were investigated. The tolerance limit was defined as the maximum concentration of influence substances that caused  $\pm 5\%$  relative error. Experimental results demonstrated that some inorganic metal ions such as

Hg<sup>2+</sup>, Mn<sup>2+</sup>, Al<sup>3+</sup>, and Ag<sup>+</sup> (100 times) showed no interference in the determination of rutin (1.0 μmol·L<sup>-1</sup>) in PBS (pH 5.0), proving the relatively good selectivity.

### 3.5 Actual sample analysis

To demonstrate the feasibility of the proposed method, the concentration of rutin in real samples (rutin tablet) was detected. The drug tablets were dissolved in ethanol and diluted by PBS (pH 5.0) to get the sample solution, which was analyzed by the procedure. The results obtained by the working curves and standard addition method are shown in Table 2. The satisfactory recoveries of rutin proves the potential application in real sample detection.

**Table 2.** Detection of rutin content in tablet by GR-NH<sub>2</sub>/DPC/GCE

Sample	Detected (μmol·L <sup>-1</sup> )	Added (μmol·L <sup>-1</sup> )	Found (μmol·L <sup>-1</sup> )	Recovery (%)
rutin	0.80	0.20	1.02	110.0
		0.40	1.23	107.5
		0.60	1.42	103.3

## 4. CONCLUSION

In the work, ZIF-8 derived porous carbon was papered and mixed with aminated graphene to obtain a nanocomposite, which was modified on GCE surface and used to investigate the electrochemical behaviors of rutin with an enhanced response. The result can be ascribed to the excellent pore structure of DPC with silk like GR nanosheet, which can be used to sensitive electrochemical detection of rutin with fast electron transfer path. By using SWV, GR-NH<sub>2</sub>/DPC/GCE exhibited the practical usage for rutin and rutin tablet analysis. This study might increase the understanding of the electrochemical properties of rutin and expand the application of novel carbon nanomaterials in electrochemical sensors.

## ACKNOWLEDGEMENTS

This work is supported by Scientific Research Projects of Higher Education Institutions in Hainan Province (Hnky2020ZD-12), the Open Foundation of Key Laboratory of Laser Technology and Optoelectronic Functional Materials of Hainan Province (2022LTOM02).

## References

1. Y.M. Li, Z.Y. Pu, Q.M. Sun, N. Pan, *Journal of Energy Chemistry*, 60(2021) 572-590.
2. X.M Wu, Z.X. Zhang, H. Soleymanabadi, *Solid State Communications*, 306(2020) 113770.
3. J. Bai, P.F. Qi, X.T. Ding, H.M. Zhang, *RSC Advances*, 6(2016) 11250-11255.
4. Q. Li, Y.Q. Zhu, S.J. Eichhor, *Journal of Materials Science*, 53(2018) 14598-14607.
5. A.R. Sk, M. Shahadat, S. Basu, Z.A. Shaikh, S.W. Ali, *Ionics*, 25(2019) 2857-2864.
6. Y. Sun, R.W. Yi, Y.C. Zhao, C.G. Liu, Y.D. Yuan, X.W. Geng, W.X. Li, Z.C. Feng, I. Mitrovic, L.

- Yang, C.Z. Zhao, *Journal of Alloys and Compounds*, 859(2021) 158347.
7. R.Y. Zou, L. Zhu, L.J. Yan, B. Shao, H. Cheng, W. Sun, *Materials Chemistry and Physics*, 266(2021) 124556.
  8. F. Marpaung, M.J. Kim, J.H. Khan, K. Konstantinov, Y. Yamauchi, Md. Shahriar, A. Hossain, J. Na, J. Kim, *Chemistry-an Asian journal*, 14(2019) 1331-1343.
  9. T. Ma, H.B. Li, J.G. Ma, P. Cheng, *Dalton Transactions*, 49(2020) 17121-17129.
  10. K. Shen, X.D. Chen, J.Y. Chen, Y.W. Li, *ACS Catalysis*, 6(2016) 5887-5903.
  11. Q. Xu, R.Q. Qiu, H. Jiang, X.M. Wang, *Journal of Electroanalytical Chemistry*, 839(2019) 247-255.
  12. W. Feng, Y.M. Wang, J.C. Chen, B.Q. Li, L.X. Guo, J.H. Ouyang, D.C. Jia, Y. Zhou, *Journal of Materials Chemistry C*, 6(2018) 10-18.
  13. W. Zhang, B. Wang, H. Luo, F. Jin, T.T. Ruan, D.L. Wang, *Journal of Alloys and Compounds*, 803(2019) 664-670.
  14. L.L. Fan, X.X. Du, S.N. Zhou, P. Yang, M.F. Li, Z.X. Kang, H.L. Guo, W.D. Fan, W.P. Kang, L. Zhang, X.Q. Lu, D.F. Sun, *Electrochimica Acta*, 317(2019) 173-181.
  15. H.B. Xu, S.H. Zhou, L.L. Xiao, H.H. Wang, S.Z. Li, Q.H. Yuan, *Journal of Materials Chemistry C*, 7(2015) 291-297.
  16. S.W. Liu, H.M. Zhang, Q. Zhao, X. Zhang, R.R. Liu, X. Ge, G.Z. Wang, H.J. Zhao, W.P. Cai, *Carbon*, 106 (2016) 74-83.
  17. Y. Hou, T.Z. Huang, Z.H. Wen, S. Mao, S.M. Cui, J.H. Chen, *Advanced energy materials*, 4(2014) 1400337.
  18. Y.Y. Niu, X.Y. Li, H. Xie, G.L. Luo, R.Y. Zou, Y.R. Xi, G.J. Li, W. Sun, *Journal of the Chinese Chemical Society*, 67(2020) 1054-1061.
  19. Y.X. Sun, B.L. Wang, Y. Deng, H. Cheng, X.Q. Li, L.J. Yan, G.J. Li, W. Sun, *Journal of the Chinese Chemical Society*, 68( 2021) 2326.
  20. Y. Vlamidis, I. Gualandi, D. Tonelli, *Journal of Electroanalytical Chemistry*, 799(2017) 285-292.
  21. G.L. Luo, X.P. Zhang, B.H. Li, B.X. Zhang, Y. Zhang, W. Sun, *J. Hainan Normal University (Natural Sci.)*, 33(2020) 24-29.
  22. P. Sukhrovov, S. Numonov, X. Mamat, *International Journal of Electrochemical Science*, 93(2018) 6550-6564.
  23. K.S. Park, Z. Ni, A.P. Côté, J.Y. Choi, R.D. Huang, F.J. Uribe-Romo, H.K. Chae, M. O’Keeffe, O.M. Yaghi, *Proceedings of the National Academy of Sciences of the United State America*, 103(2006) 10186-10191.
  24. G.L. Luo, Y. Deng, X.P. Zhang, R.Y. Zou, W. Sun, Y.B. Wang, G.J. Li, *New Journal of Chemistry*, 43(2019) 16819.
  25. P.D. Du, N.T. Hieu, T.V. Thien, *Journal of Nanomaterials*, 12(2021) 9988998.
  26. S.L. Yang, G. Li, J. Feng, P.Y. Wang, L.B. Qu, *Electrochimica Acta*, 412(2022) 140157.
  27. G.L. Luo, R.Y. Zou, Y.Y. Niu, Y. Zhang, B.X. Zhang, J. Liu, G.J. Li, W. Sun, *Journal of Pharmaceutical and Biomedical Analysis*, 190(2020) 113505.
  28. J. Liu, W.J. Weng, C.X. Yin, X.B. Li, Y.Y. Niu, G.J. Li, W. Sun, *Journal of the Chinese Chemical Society*, 66(2019) 1336-1340.
  29. Q. He, Y. Wu, Y. Tian, G. Li, J. Liu, P. Deng, D. Chen, *Nanomaterials*, 9(2019) 115.
  30. M.B. Gholivand, L. Mohammadi-Behzad, H. Hosseinkhani, *Analytical biochemistry*, 493(2016) 35-43.
  31. E. Laviron, *Electroanalytical Chemistry and Interracial Electrochemistry*, 52(1974) 355-393.
  32. D. Saritha, A.R. Koirala, M. Venu, G. Dinneswara Reddy, A. Vijaya Bhaskar Reddy, G. Madhavi, *Electrochimica Acta*, 313(2019) 523-531.
  33. Q. Gong, H. Han, Y. Wang, C. Yao, H. Yang, J. Qiao, *New Carbon Materials*, 35(2020) 34-41.
  34. L. Liu, Y. Gou, X. Gao, P. Zhang, W. Chen, S. Feng, F. Hu, Y. Li, *Materials Science and Engineering C*, 42(2014) 227-233.

35. H.F. Bagheri, M. Arvand, M.F. Habibi, *Microchemical Journal*, 181(2022) 107712.
36. S.L. Yang, G. Li, J. Feng, P.Y. Wang, L.B. Qu, *Electrochimica Acta*, 412(2022) 140157.
37. G.L. Luo, R.Y. Zou, Y.Y. Niu, Y. Zhang, B.X. Zhang, J. Liu, G.J. Li, W. Sun, *Journal of Pharmaceutical and Biomedical Analysis*, 190(2020) 113505.
38. J. Liu, W.J. Weng, C.X. Yin, X.B. Li, Y.Y. Niu, G.J. Li, W. Sun, *Journal of the Chinese Chemical Society*, 66(2019) 1336-1340.
39. H. Cheng, J. Liu, Y.X. Sun, T. Zhou, Q.Y. Yang, S.Y. Zhang, X.P. Zhang, G.J. Li, W. Sun, *RSC Advances*, 10(2020) 42340-42348.
40. L.J. Yan, T.X. Hu, X.Q. Li, F.Z. Ding, B. Wang, B.L. Wang, B.X. Zhang, F. Shi, W. Sun, *Electroanalysis*, 34(2021) 286-293.
41. P. Kaleeswarran, C. Koventhan, S.M. Chen, A. Arumugam, *Colloids and Surfaces A: Physicochemical and Engineering Aspects*, 643(2022) 128740.
42. A. Şenocak, V.Sanko, S. Tümay, Y. Orooji, E. Demirbas, Y.J. Yoon, A.K. Affiliation, *Food and Chemical Toxicology*, 164(2022) 113016.
43. J. Lou, L.J. Yan, W.C. Wang, C.X. Ruan, A.H.Hu, W. Sun, *Journal of the Chinese Chemical Society*, 62(2015) 640-646.
44. Y.X. Lu, J. Hu, Y.B. Zeng, Y. Zhu, H.L. Wang, X.L. Lei, S.S. Huang, L.H. Guo, L. Li, *Sensors and Actuators B: Chemical*, 311(2020) 127911.
45. X.H. Liu, L. Li, X.P. Zhao, X.Q. Lu, *Colloids and Surfaces B: Biointerfaces*, 81(2010) 344-349.

© 2022 The Authors. Published by ESG ([www.electrochemsci.org](http://www.electrochemsci.org)). This article is an open access article distributed under the terms and conditions of the Creative Commons Attribution license (<http://creativecommons.org/licenses/by/4.0/>).